JMEPEG (2019) 28:7198–7205
https://doi.org/10.1007/s11665-019-04461-w

1059-9495/$19.00

Fabrication and Properties of (Ti, W, Mo, Nb, Ta)(C, N)-Co-Ni Cermets

Houan Zhang, Ming Fu, Lili Ma, Siyong Gu, Jiawei Liu, and Ying Chen

(Submitted March 30, 2019; in revised form August 8, 2019; published online November 20, 2019)

Fine single-phase (Ti, W, Mo, Nb, Ta)(C, N) solid solution powders were synthesized through the carbothermal reduction method. (Ti, W, Mo, Nb, Ta)(C, N)-Co-Ni cermets were fabricated via vacuum sintering. Micrographs of powders and microstructures of the cermets were observed using transmission electron microscopy and scanning electron microscopy in combination with energy-dispersive spectroscopy. Phase compositions were investigated using x-ray diffraction. The C and N contents were measured using elemental analysis (CHNS/O). The optimized conditions for the synthesis process of single-phase (Ti, W, Mo, Nb, Ta)(C, N) solid solution powders with high nitrogen content were 1500 °C for 2 h under a 2 kPa nitrogen atmosphere. Under such conditions, the particle size of the synthesized powder was less than 140 nm, and its carbon and nitrogen contents were 9.174 and 7.040 wt.%, respectively. The synthesized fine (Ti, W, Mo, Nb, Ta)(C, N) solid solution powders had a significant positive impact on the strengthening and hardening of Ti(C, N)-based cermets. The values of hardness and transverse rupture strength of the (Ti, W, Mo, Nb, Ta)(C, N)-Co-Ni cermets sintered at 1450 °C for 1 h in vacuum (SSC3) increase by 14.7 and 20.2% compared to those of traditional Ti(C, N)-WC-Mo_2C-NbC-TaC-Co-Ni cermet (TC), respectively. However, the K_{IC} value of SSC3 decreases by 14.1% compared to that of TC. The mechanism of strengthening and hardening and the cause of the low fracture toughness of the SSC were revealed by comparing the differences in the microstructures of SSC and TC.

Keywords electron microscopy, powder metallurgy, sintering, x-ray

1. Introduction

Ti(C, N)-based cermets are advanced cutting tool materials that have been developed from TiC-based cermets. Because of their high red-hardness, excellent chemical resistance, and good resistance to temperature oxidation, Ti(C, N)-based cermets are widely used in automobile manufacturing, aerospace industries, and other fields (Ref 1-4). For complex cutting environments, the low flexural strength restricts the application of Ti(C, N)-based cermets. Traditional Ti(C, N)-based cermets are usually fabricated from mixtures of Ti(C, N), Co, Ni, and other carbides powders by steps, such as ball-milling, compaction, and sintering. Additions of carbides (i.e., WC, Mo_2C, TaC, NbC, etc.) improve the mechanical properties of Ti(C, N)-based cermets (Ref 5-7). However, after added carbides, it is difficult to control the solid solution during sintering process. As a result, this process increases the strain at the interfaces between the core and rim, and this can impair the mechanical properties of the materials (Ref 8, 9). It was recently reported that using the solid solution powders of (Ti, Ta, W)(C, N) improved the mechanical properties of the cermets (Ref 3, 10, 11). Jin et al. used TiO_2, WO_3, MoO_3, V_2O_5, NiO, and carbon black powders as raw materials and synthesized (Ti, W, Mo, V)(C, N)-Ni cermet powders via a conventional carbothermal reduction–nitridation reaction (Ref 11, 12). TiO_2, WO_3, MoO_3, NiO, Co_3O_4, and carbon black powders had been used as starting materials, and ultrafine (Ti, W, Mo)(C, N)-(Ni, Co) cermet powders were produced at a lower temperature via a spark plasma-assisted carbothermal reduction–nitridation reaction (Ref 13). Meanwhile, previous work showed that using fine raw powders could increase the hardness and decrease the toughness of Ti(C, N)-based cermets (Ref 14). However, rare publications have a deep insight on the comprehensive effect of the solid solution of W, Mo, Nb, and Ta elements and fine powders on the property and microstructure of Ti(C, N)-based cermets. Therefore, in this article, fine (Ti, W, Mo, Nb, Ta)(C, N) solid solution powders are synthesized via the carbothermal reduction method, and the effects on the microstructures and properties of Ti(C, N)-based cermets are investigated.

Houan Zhang, Ming Fu, Lili Ma, Siyong Gu, Jiawei Liu, and **Ying Chen**, Fujian Province Key Laboratory of Functional Materials and Applications, Xiamen University of Technology, Xiamen 3610?4 Fujian, People's Republic of China; and Xiamen Key Laboratory for Powder Metallurgy Technology and Advanced Materials, Xiamen University of Technology, Xiamen 361024 Fujian, People's Republic of China. Contact e-mail: ha_zhang@163.com.

2. Experimental Procedures

2.1 Materials

TiO_2 powders (0.2-0.5 μm), WO_3 powders (0.2 μm), MoO_3 powders (2-5 μm), Nb_2O_5 powders (1 μm), Ta_2O_5 powders (0.5 μm), carbon black powders (0.1 μm), Ti($C_{0.7}$, $N_{0.3}$) powders (<1.0 μm), WC powders (<1.0 μm), Mo_2C powders (<1.0 μm), TaC powders (<1.0 μm), NbC powders (<1.0 μm), Co powders (0.8 μm), and Ni powders (0.8 μm) were used as raw materials. All of the raw materials were 99.9% in purity and were purchased from Beijing Hongyu Co., Ltd., China.

2.2 Synthesis of Solid Solution Powders

Using the chemical composition (in weight) of 50% TiO_2-25% C-12% WO_3-5% MoO_3-4% Nb_2O_5-4% Ta_2O_5, the powders were first mixed in a planetary ball mill for 4 h using ZrO_2 balls at a speed of 200 r/min. The mixtures were then dried. Finally, the mixtures were heated in a tubular furnace at different conditions (temperatures in the range of 1300-1600 °C for 1-3 h under a N_2 atmosphere) to synthesize (Ti, W, Mo, Nb, Ta)(C, N) solid solution powders with a C/N ratio of 7:3 using the carbothermal reduction method. Then, the powders were cooled naturally to room temperature in a furnace that was cooled under a N_2 atmosphere. In all of the experimental runs, a pressure of 1-2 kPa in a N_2 atmosphere (99.9% purity) was maintained.

2.3 Preparation of (Ti, W, Mo, Nb, Ta)(C, N)-Co-Ni Cermets

According to the chemical composition (in weight) of 85% (Ti, W, Mo, Nb, Ta)(C, N)-7.5% Co-7.5% Ni, powders of (Ti, W, Mo, Nb, Ta)(C, N) were synthesized at 1500 °C for 2 h under a N_2 pressure of 2 kPa, and powders of Co and Ni were milled and mixed in a planetary ball mill for 24 h using WC balls at a speed of 135 r/min. Then, the mixed powders were sieved using a mesh of size 0.125 mm and dried in a vacuum drying oven at 90 °C for 2 h. The dry mixtures were pressed in a rectangular beam-shaped die at a uniaxial pressure of 250 MPa. Finally, the (Ti, W, Mo, Nb, Ta)(C, N)-Co-Ni cermets (named SSC) were sintered in a ZSJ-20X20X20 vacuum oven at 1350-1550 °C for 10 min-8 h in vacuum. After sintering, the samples were cooled in vacuum to room temperature in the furnace. For comparison, the traditional Ti (C, N)-WC-Mo_2C-NbC-TaC-Co-Ni cermet (named TC) was prepared using the same sintering process and target composition (in weight) with 65% Ti($C_{0.7}$, $N_{0.3}$), 17% WC, 6% Mo_2C, 6% TaC, 6% NbC, 7.5% Co, and 7.5% Ni raw powders.

2.4 Characterization

The sintering samples were polished with SiC papers and 3-μm diamond pastes. The density of the specimen was measured according to Archimedes' law. Hardness (HV_{30}) values of the sintering samples were measured on a Vickers hardness tester using 298 N for 10 s according to the GB/T 7997–2014 standard. Indentation fracture toughness (K_{IC}) was calculated using the Vickers hardness following Eq 1 (Ref 15):

$$K_{IC} = 0.15\sqrt{\frac{HV_{30}}{\sum_{i=1}^{4} l_i}} \quad \text{(Eq 1)}$$

where HV_{30} is the Vickers hardness (N/mm^2) and l_i is the length of the crack tip from the hardness indentation (mm). Transverse rupture strength (TRS) was tested according to the ISO 3327:2009 standards. The test pieces had dimensions of 5.5 mm × 6.5 mm × 20.0 mm, and the test span was a length of 12.0 mm. All of the data are reported as the average value of five measured values. The morphology and particle sizes of the synthesized powders and microstructures of the cermets were observed using a scanning electron microscope (FE-SEM, Zeiss sigma 500, Germany) equipped with an energy-dispersive spectroscope (EDS, Oxford Instrument X-maxN, UK). A transmission electron microscope (TEM) was operated at 200 kV (FEI Talos F200 TEM/STEM, USA). The phase composition was investigated using an x-ray diffractometer (XRD, PANalytical X′Pert PRO, Netherland). The C and N contents were measured using an element analyzer (Vario ELIII, CHNS/O, Germany).

3. Results and Discussion

3.1 Synthesis of the (Ti, W, Mo, Nb, Ta)(C, N) Solid Solution Powders

Figure 1(a) shows the XRD patterns of the mixed powders. It can be seen that the mixed powder still retained the same phase composition as the raw material (TiO_2, WO_3, MoO_3, Nb_2O_5, and Ta_2O_5). Because the carbon black was amorphous, it was not found, as seen in Fig. 1(a). The powders synthesized

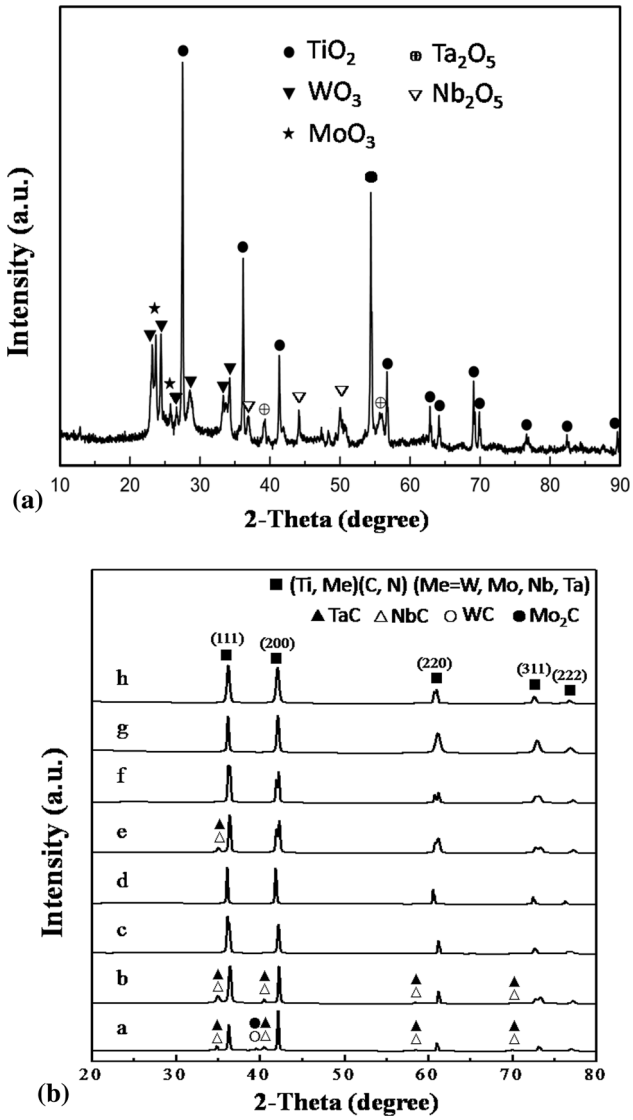

Fig. 1 XRD patterns of the mixed powders (a) and synthesized (b) powders at different conditions (temperature, time, and nitrogen pressure in order). (a) 1300 °C, 3 h, 2 kPa; (b) 1400 °C, 3 h, 2 kPa; (c) 1500 °C, 3 h, 2 kPa; (d) 1600 °C, 3 h, 2 kPa; (e) 1500 °C, 1 h, 2 kPa; (f) 1500 °C, 2 h, 2 kPa; (g) 1500 °C, 3 h, 1 kPa; (h) 1500 °C, 3 h, 1.5 kPa

via carbothermal reduction at different temperatures, durations of time, and pressures in a N_2 atmosphere are shown in Fig. 1 (b). Comparing a with b, c, and d in Fig. 1(b), it can be seen that the (Ti, Me)(C, N) phase (where Me is W, Mo, Nb, and Ta) formed, but there are also some peaks that correspond to WC, Mo_2C, TaC, and NbC at 1300 °C. With an increase in temperature, the peaks for WC and Mo_2C disappeared, and a few peaks for TaC and NbC were still present at 1400 °C for 3 h. When the temperature was increased above 1500 °C for 3 h [c and d in Fig. 1(b)], all of the peaks for the TaC and NbC phases disappeared, whereas only a single (Ti, Me)(C, N) phase was identified. Similar results were also found for fabricated samples shown in f, g, and h of Fig. 1(b). However, there are a few peaks for TaC and NbC that still appeared at 1500 °C for 1 h at 2 kPa [e in Fig. 1(b)]. This indicates that single-phase (Ti, W, Mo, Nb, Ta)(C, N) solid solution powders were synthesized at 1500 °C for at least 2 h under N_2 in this experiment. As seen in Fig. 1(b), the solid solubility of atoms of tungsten and molybdenum in Ti(C, N) was better than that of niobium and tantalum atoms. Meanwhile, when the temperature was increased from 1300 to 1500 °C for 3 h, the intensity ratio of the (111) and (200) peaks for the Ti(C, N)-based solid solution phase increased from 0.996 to 1.15, which was higher than that for $Ti(C_{0.7}N_{0.3})$ (0.510, JCPDS42-1489). This can be interpreted to mean that the W, Mo, Nb, and Ta atoms were easier to replace Ti atoms in the (111) crystal plane than in the (200) crystal plane, and this leads to an increase in the ratio. During the carbothermal reduction reaction process, the oxides of W, Mo, Ta, and Nb reacted with C to form WC, Mo_2C, TaC, NbC, and CO (Ref 16). Meanwhile, under the combined action of a TiO_2/C solid–solid reaction and a solid–gas reaction mainly between oxides and CO, C, CO_2, and N_2 (Ref 16-18), Ti(C, N) was synthesized at 750-1300 °C according to the following reaction sequences: TiO_2 (anatase)→TiO_2(rutile)→Ti_nO_{2n-1} ($n\geq4$)→Ti_3O_5→Ti(N, O)→Ti(C, N, O)→Ti(C, N). Then, with the increase in temperature, atoms of W, Mo, and Ta, Nb successively diffused in Ti(C, N) unit cells, and finally, the (Ti, W, Mo, Nb, Ta)(C, N) solid solution phase was formed.

The C and N contents of the powders that were synthesized at different temperatures, durations of time, and pressures in a N_2 atmosphere are listed in Table 1. With an increase in the synthesis temperature, the C content first decreased (from 1300 to 1400 °C) and then increased (over 1400 °C). However, the N content was the opposite. When the duration of the holding time was increased, the C increased and N contents decreased. With an increase in the N_2 pressure from 1 to 2 kPa, the C content decreased, and the N content increased. These observations indicate that a higher N_2 pressure and shorter holding time in the reaction system would result in higher N content in (Ti, W, Mo, Nb, Ta)(C, N) solid solution powders. Table 1 also shows the lattice parameters of the powders that were synthesized at different conditions. It can be seen that the lattice parameters increased with increases in the reduction temperature, duration of holding time, and N_2 pressure. This is mainly attributable to the diffusion of W, Mo, Nb, and Ta atoms. Atoms of these elements have larger atomic radii, and this leads to the expansion of the Ti(C, N) crystal lattice. When the powders were synthesized at 1600 °C for 3 h under a N_2 pressure of 2 kPa, the solid solution powders had a higher lattice parameter, but the N content was obviously reduced because more and more N atoms were replaced by C atoms, and

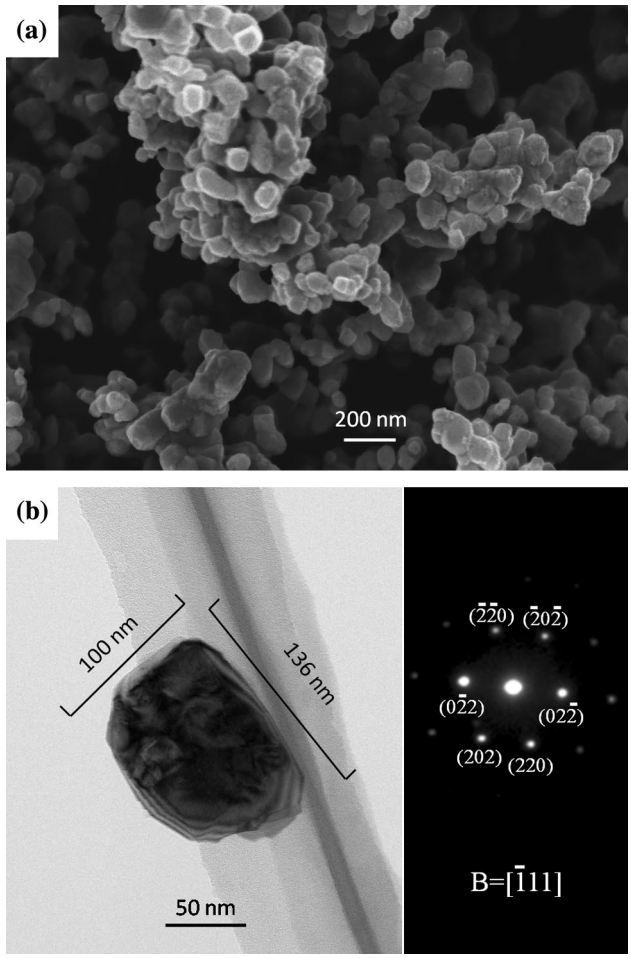

Fig. 2 Micrographs of the (Ti, W, Mo, Nb, Ta)(C, N) solid solution powders synthesized at 1500 °C for 2 h under 2 kPa N_2 pressure. (a) SEM; (b) TEM (BF) with SAD in the lower left corner

Table 1 The C and N contents, lattice parameters of the synthesized powders

Temperature, °C	Time, h	Nitrogen pressure, kPa	C content, wt.%	N content, wt.%	Lattice constant, Å
1300	3	2	9.516	6.076	4.2700
1400	3	2	8.803	7.300	4.2830
1500	3	2	9.632	6.482	4.2967
1600	3	2	12.910	2.677	4.3180
1500	2	2	9.174	7.040	4.2829
1500	1	2	9.056	7.217	4.2825
1500	3	1.5	10.300	5.600	4.2940
1500	3	1	11.500	4.600	4.2918

this led to the outgassing of nitrogen atoms at higher temperature (Ref 13).

From Fig. 1(b) and Table 1, it is concluded in this experiment that the powders should be synthesized at 1500 °C for 2 h under a N_2 pressure of 2 kPa to obtain single-phase (Ti, W, Mo, Nb, Ta)(C, N) solid solution powders with a higher nitrogen content. Under such synthesis conditions, the carbon and nitrogen contents of the powders were 9.174 and 7.040 wt.%, respectively. No free C was found, and the oxygen content was 0.54% in these synthesized powders. Micrographs of the synthesized powders are shown in Fig. 2. As seen in Fig. 2(a), the size of the powder particles was almost uniform. Figure 2(b) shows that the length and width of a particle were about 136 and 100 nm, respectively. According to the literature (Ref 17, 18), the carbothermal reduction reaction proceeds primarily on the external surface of the carbon particles, and the synthesized powders gradually became finer with uniform particles and the formation of a cubic phase. The formation of titanium carbonitride via carbothermal reduction of titanium dioxide is a complex process that includes crystal transformation and chemical reaction. This process promotes the transformation of the raw coarse titanium dioxide particles into fine titanium carbonitride powders. Selected area electron diffraction (SAD) patterns of the particle shows the {220} crystal facet in the [$\bar{1}$11] zone axis of a face-center cubic structure, and this is in accordance with the Ti(C, N) result (PDF card number JCPDS 42-1489). This means that only a one-phase

Table 2 Mechanical properties of cermets

Cermets	Sintering condition		Relative density, %	Mechanical properties		
	Temperature, °C	Holding time, min		HV_{30}, kg/mm^2	TRS, MPa	K_{IC}, MPsa·m$^{1/2}$
SSC1	1350	60	91.4	1581±45	1300±21	4.86±0.25
SSC2	1400	60	97.7	1690±53	1530±32	8.51±0.12
SSC3	1450	60	99.3	1787±48	1550±26	8.94±0.16
SSC4	1500	60	98.8	1684±55	1240±23	8.32±0.10
SSC5	1550	60	98.3	1578±45	1100±35	8.14±0.11
SSC31	1450	10	93.9	1679±43	1260±30	8.36±0.18
SSC32	1450	180	99.2	1777±52	1340±28	8.74±0.09
SSC33	1450	300	98.9	1710±46	1190±31	8.69±0.10
SSC34	1450	480	98.2	1704±43	1000±26	8.65±0.11
TC	1450	60	98.0	1558±51	1290±36	10.2±0.12

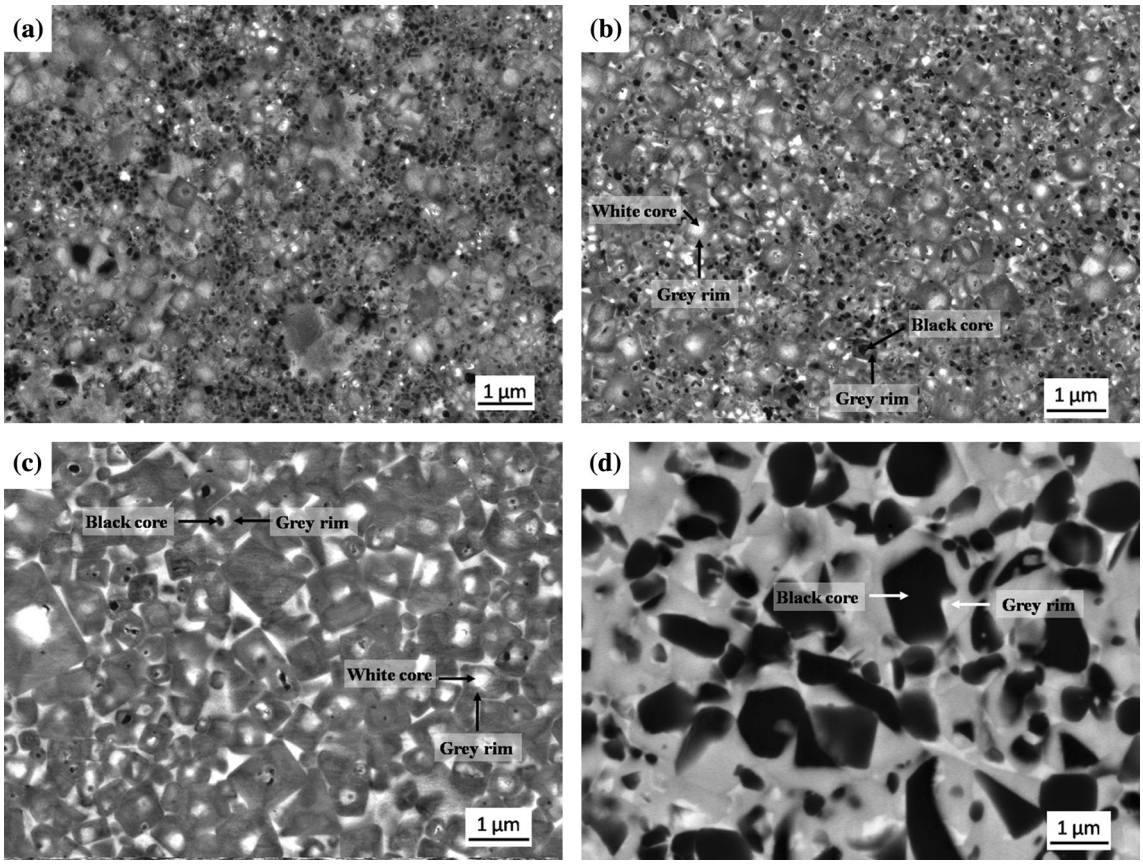

Fig. 3 BSE images of the microstructure of the Ti(C, N)-based cermets. (a) SSC1; (b) SSC3; (c) SSC5; (d) TC

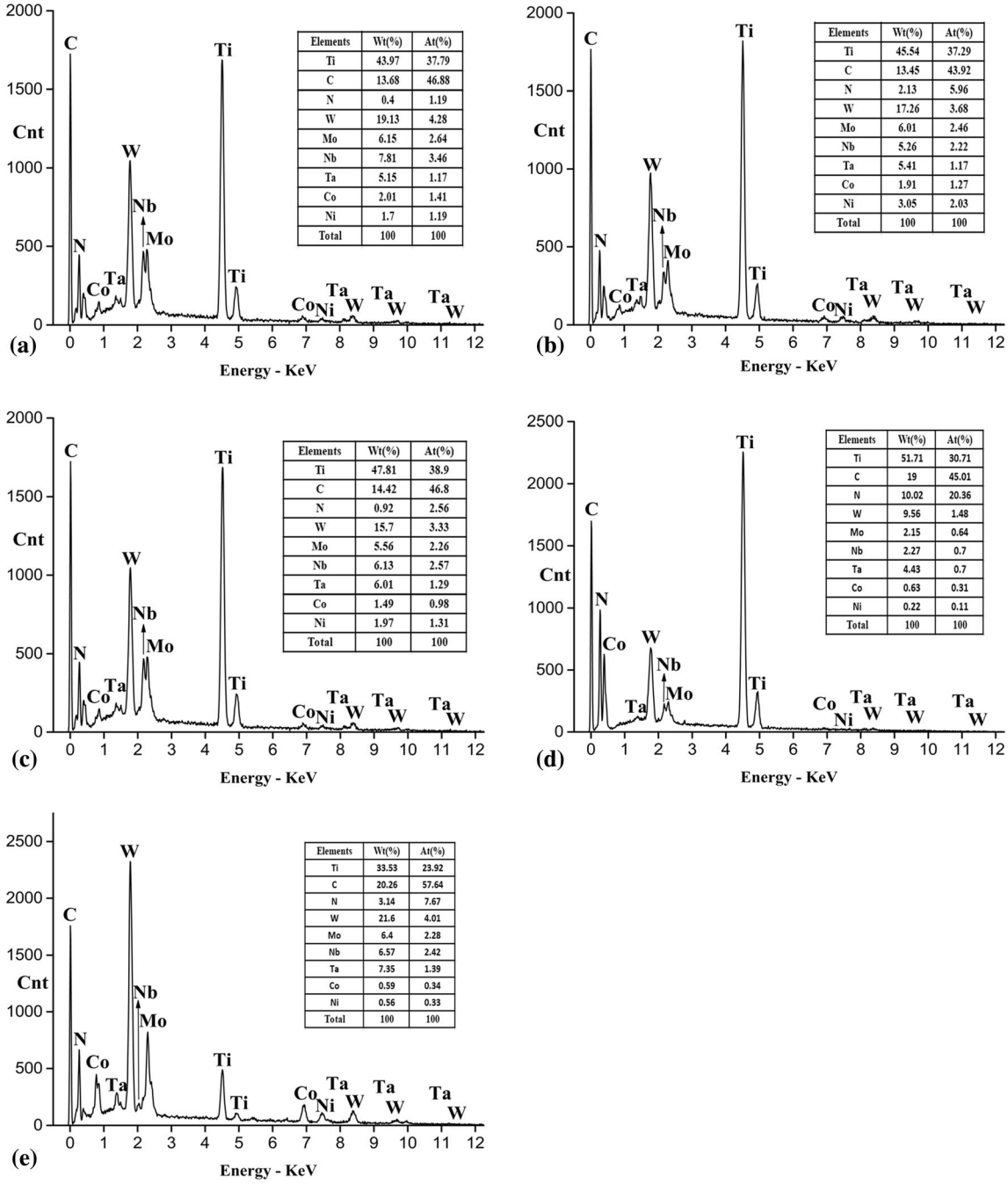

Fig. 4 The EDS spectrums of white core (a)–gray rim (b), black core (c) of sample SSC, and black core (d)–gray rim (e) of sample TC in Fig. 3

solid solution was present in the synthesized powders, and this indicates that the solid solution of W, Mo, Ta, and Nb elements did not change the structure of the Ti(C, N) solid solution.

3.2 Mechanical Properties of (Ti, W, Mo, Nb, Ta)(C, N)-Co-Ni Cermets

Mechanical properties of the (Ti, W, Mo, Nb, Ta)(C, N)-Co-Ni cermets that were sintered at different temperatures and durations of holding time are listed in Table 2. It can be seen that the HV_{30}, TRS, and K_{IC} values of SSC first increased and then decreased when the sintering temperature and duration of holding time increased. When sintered at 1450 °C for 60 min (sample numbered SSC3), the HV_{30}, TRS, and K_{IC} values of SSC3 were higher than those of the other SSC samples. These values were 1787 kg/mm^2, 1550 MPa, and 8.94 MPa m$^{1/2}$, respectively. Compared with the properties of TC, the hardness of SSC3 was improved by 14.7%, and the TRS was improved by 20.2%. This indicates that fine (Ti, W, Mo, Nb, Ta)(C, N) solid solution powders are beneficial for increasing the hardness and strength of the Ti(C, N)-based cermets. However,

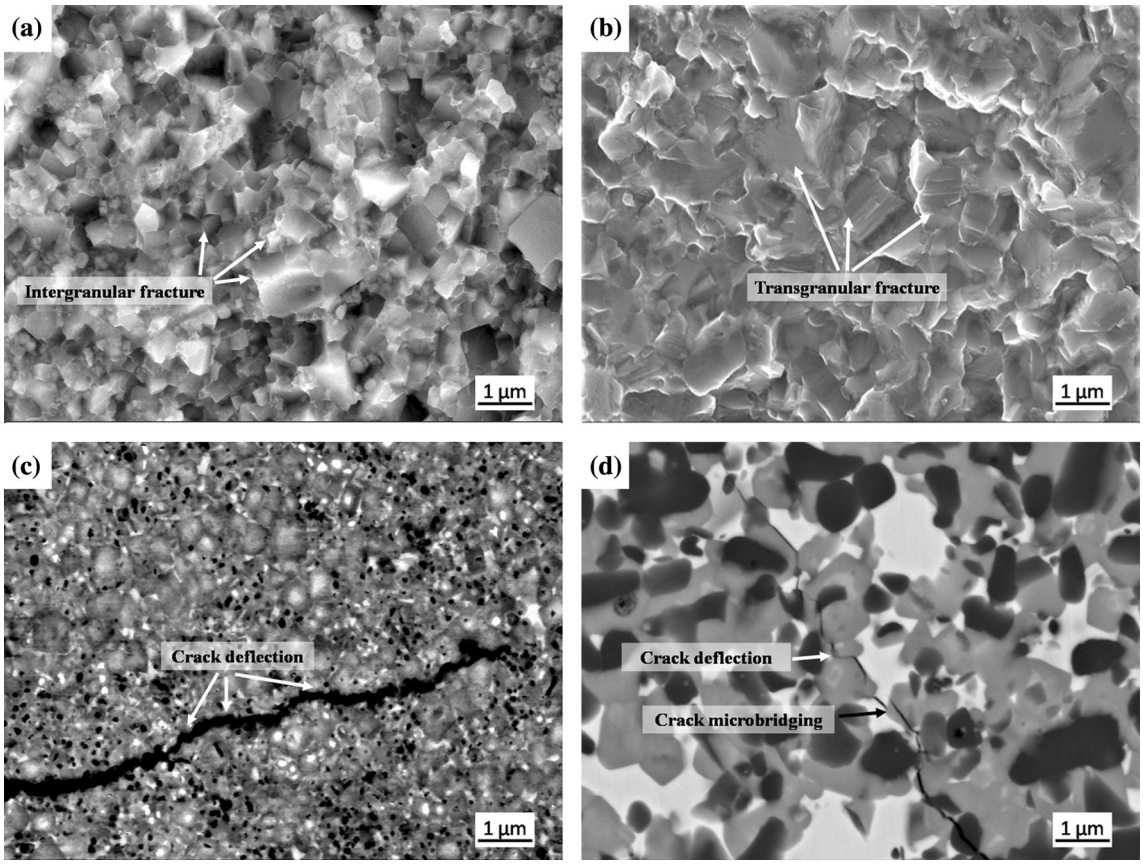

Fig. 5 SEM micrographs of the fracture surface and crack propagation of samples of SSC3 and TC. (a) Fracture surface of SSC3; (b) fracture surface of TC; (c) crack propagation of SSC3; (d) crack propagation of sample TC

the fracture toughness of SSC3 was 14.1% lower than that of TC.

3.3 Microstructures of (Ti, W, Mo, Nb, Ta)(C, N)-Co-Ni Cermets

Figure 3 shows BSE images of the SSC and TC cermets. In Fig. 3(a), it can be seen that the "core–rim" microstructures in the SSC1 samples that were sintered at 1350 °C started to form, but there were still many fine pores that resulted in relatively low density. This can be attributed to the low sintering temperature and the short sintering time, which resulted in insufficient dissolution–precipitation during liquid-phase sintering (Ref 19, 20). When samples were sintered at 1450 °C for 60 min, the microstructures of SSC3 were a fine white core surrounded by a gray rim and a fine black core with a gray rim (Fig. 3b). These findings are similar to the microstructures described in Ref 21, 22. With an increase in the sintering temperature, the core–rim microstructures grew, and the number of black cores in sample SSC5 decreased (Fig. 3c). Similar changes were also found in the SSC32, SSC33, and SSC34 samples with longer holding time when sintered at 1450 °C. EDS analysis of SSC3 and TC samples were carried out in Fig. 4. The core–rim microstructures of Ti(C, N)-based cermets formed through a dissolution and precipitation process during liquid-phase sintering. The starting powders to synthesize SSC consisted of the solid solution phase of (Ti, W, Mo, Nb, Ta)(C, N) and the binder phases of Co and Ni. During the sintering process, the solid solution phase gradually dissolved into the binder phase and formed the gray rim. Compared with Fig. 4(b) and (c), Fig. 4(a) shows that the white core in Fig. 3(b) had a high tungsten content and low titanium content. The black core had high titanium content and low tungsten content in Fig. 4(c). With an increase in the sintering temperature or with extended sintering time, the fine black core gradually dissolved, and the volume of the black core gradually deceased. Therefore, a few coreless microstructures are found in Fig. 3(c). In comparing the SSC materials, SSC3 had finer microstructures [<1 μm in size, as seen in Fig. 3(b)] than that in other SSC samples, and this resulted in higher hardness and strength, according to the well-established Hall–Petch strengthening and hardening relationship. In contrast, the gray rim phase was brittle, and the thin gray rim of the surrounding white core in the SSC3 sample was also advantageous for improving the TRS and K_{IC} values of the matrix. Therefore, the hardness, transverse rupture strength, and fracture toughness of the SSC3 sample were higher than that of the other SSC materials.

Micrographs of the fracture surface and crack propagation of samples of SSC3 and TC are shown in Fig. 5. It can be seen from Fig. 5(a) and (b) that the fracture surface of SSC3 was mainly intergranular fracture, but the fracture surface of TC was mainly transgranular fracture. The K_{IC} value of cermet is related to both the hard phase and binder phase (Ref 23). Because the (Ti, Me)(C, N) phase intrinsically has better elastic properties than the Ti(C, N) phase (Ref 24), an increase in the (Ti, Me)(C, N) core content improves the toughness of the hard phase. Meanwhile, a decrease in the grain size resulted in fine

grain strengthening (Ref 25). As shown in Fig. 3(b), SSC3 has high and fine (Ti, W, Mo, Nb, Ta)(C, N) core content; it improves the toughness and strength of the hard phase. Therefore, cracks in SSC3 mainly propagate along grain boundaries, as seen in Fig. 5(a). The large binder mean free path and the increase in the W content in the rims in the Ti(C, N) base cermets helped improve the fracture toughness (Ref 23, 25, 26). As seen in Figs. 3(d) and 4(e), TC had coarse black core–gray rim microstructures and high W content in thick gray rims, and this led to an increase in the binder mean free path and an increase in the W content in the rim, which improved the toughness. Only crack deflection along the crack propagation path is observed in Fig. 5(c). However, crack deflection and crack microbridging are observed in Fig. 5(d), and this is attributed to the longer mean free path caused by grain coarsening in TC. This also led to an improvement in the toughness of TC.

4. Conclusions

Fine (Ti, W, Mo, Nb, Ta)(C, N) solid solution powders were successfully synthesized via the carbothermal reduction method. The mechanical properties and microstructures of the (Ti, W, Mo, Nb, Ta)(C, N)-Co-Ni cermets were studied, and the following conclusions can be drawn from the present investigations:

(1) The favorable synthesis conditions of (Ti, W, Mo, Nb, Ta)(C, N) single-phase solid solution powders with high nitrogen content are 1500 °C for 2 h under a pressure of 2 kPa in a nitrogen atmosphere. Under these conditions, the particle size of the synthesized powders is less than 140 nm, and the carbon and nitrogen contents of the powders are 9.174 and 7.040 wt.%, respectively. XRD results show that the solid solubilities of W and Mo atoms in Ti(C, N) are better than those of Nb and Ta.

(2) The optimal sintering process of (Ti, W, Mo, Nb, Ta)(C, N)-Co-Ni cermets is at 1450 °C for 1 h in vacuum. Using fine (Ti, W, Mo, Nb, Ta)(C, N) solid solution powders as the starting materials had good effects on the hardening and strengthening of Ti(C, N)-based cermets. The hardness and TRS values of SSC3 increase by 14.7 and 20.2%, respectively, compared to those of TC. However, the K_{IC} value of SSC3 decreased by 14.1% compared to that of TC.

(3) The microstructures of the (Ti, W, Mo, Nb, Ta)(C, N)-Co-Ni cermets that had fine microstructure and a thin gray rim result in high hardness and TRS. The high fracture toughness of TC is primarily attributed to crack deflection and crack microbridging, which result from the coarse black core–gray rim microstructures and high W content in the thick gray rims.

Acknowledgments

This work was financially supported by the Natural Science Foundation of Fujian Provincial of China (No. 2019J01870), the Scientific Research Fund of Xiamen City of Fujian Provincial of China (No. 3502Z20179025), and Program for Innovative Research Team in Science and Technology in Fujian Province University.

References

1. P. Ettmayer, H. Kolaska, W. Lengauer, and K. Dreyer, Ti(C, N) Cermets Metallurgy and Properties. *Int. J. Refract. Met. Hard Mater.* **13**, 343–351 (1995)
2. Y. Peng, H. Miao, and Z. Peng, Development of TiCN-Based Cermets: Mechanical Properties and Wear Mechanism. *Int. J. Refract. Met. Hard Mater.* **39**, 78–89 (2013)
3. S.W. Oh, S.Y. Ahn, K.S. Oh, H. Lee, and T.J. Chung, Investigation into the Microstructure and Cutting Performance of (Ti, Ta, W)(CN)–Co/Ni Cermets. *Int. J. Refract. Met. Hard Mater.* **53**, 36–40 (2015)
4. H. Zhang, S. Gu, and J. Yi, Fabrication and Properties of Ti(C, N) Based Cermets Reinforced by Nano-CBN Particles. *Ceram. Int.* **38**, 4587–4591 (2012)
5. H. Zhang, J. Yi, and S. Gu, Mechanical Properties and Microstructure of Ti(C, N) Based Cermets Reinforced by Nano-Si_3N_4 Particles. *Int. J. Refract. Met. Hard Mater.* **29**, 158–162 (2011)
6. C. Yi, H. Fan, J. Xiong, Z. Guo, G. Dong, W. Wan, and H. Chen, Effect of WC Content on the Microstructures and Corrosion Behavior of Ti(C, N)-Based Cermets. *Ceram. Int.* **39**, 503–509 (2013)
7. E. Chicardi, Y. Torres, J.M. Córdoba, P. Hvizdoš, and F.J. Gotor, Effect of Tantalum Content on the Microstructure and Mechanical Behavior of Cermets Based on $(Ti_xTa_{1-x})(C_{0.5}N_{0.5})$ Solid Solutions. *Mater. Des.* **53**, 435–444 (2014)
8. S.Y. Ahn and S. Kang, Formation of Core/Rim Structures in Ti(C, N)–WC–Ni Cermets via a Dissolution and Precipitation Process. *J. Am. Ceram. Soc.* **83**, 1489–1494 (2000)
9. J. Jung and S. Kang, Effect of Nano-size Powders on the Microstructure of Ti(C, N)–xWC–Ni Cermets. *J. Am. Ceram. Soc.* **90**, 2178–2183 (2007)
10. T. Matsuda and H. Matsubara, Synthesis of Titanium Carbonitride Nano-Powder by Carbothermal Reduction of TiO_2. *Int. J. Refract. Met. Hard Mater.* **42**, 1–8 (2014)
11. Y. Jin, Y. Liu, Y. Wang, and J. Ye, Study on Phase Evolution during Reaction Synthesis of Ultrafine (Ti, W, Mo, V)(CN)–Ni Composite Powders. *Mater. Chem. Phys.* **118**, 191–196 (2009)
12. Y. Jin, Y. Liu, Y.K. Wang, and J. Ye, Synthesis of Ultrafine (Ti, W, Mo, V)(C, N)–Ni Composite Powders by Low-Energy Milling and Subsequent Carbothermal Reduction–Nitridation Reaction. *J. Alloys Compd.* **486**, L34–L36 (2009)
13. H. Li, D. Xiang, Y. Cao, S. Zhao, and G. Tu, Spark Plasma Assisted Carbothermal Reduction–Nitridation Synthesis of (Ti, W, Mo)(C, N)–(Ni, Co) Powders. *Ceram. Int.* **43**, 14726–14731 (2017)
14. Y. Chai, H. Liu, C. Huang, B. Zou, and H. Liu, Study of Influencing Factors of Mechanical Properties of Ti(C, N)-Based Cermets. *Key Eng. Mater.* **589–590**, 578–583 (2013)
15. W. Wan, J. Xiong, and M. Liang, Effects of Secondary Carbides on the Microstructure, Mechanical Properties and Erosive Wear of Ti(C, N)-Based Cermets. *Ceram. Int.* **43**, 944–952 (2017)
16. P. Rong, Y. Liu, J. Ye, Q. Cao, and A. Liu, Synthesis of (Ti, W, Mo, Ta, Cr)(C, N) Solid Solution Powders by Carbothermal Reduction-Nitridation in an Open System. *J. Alloys Compd.* **718**, 425–432 (2017)
17. X. He, J.W. Ye, Y. Liu, B.Q. Chen, Z.T. Jiang, H.W. Zou, L. Deng, and M.J. Tu, Phase Transition and Microstructure Evolution during the Carbothermal Preparation of Ti(C, N) Powders in an Open System. *Adv. Powder Technol.* **21**, 448–451 (2010)
18. L.-M. Berger and W. Gruner, Investigation of the Effect of a Nitrogen-Containing Atmosphere on the Carbothermal Reduction of Titanium Dioxide. *Int. J. Refract. Met. Hard Mater.* **20**, 235–251 (2002)
19. D. Mari, S. Bolognini, G. Feusier, T. Cutard, C. Verdon, T. Viatte, and W. Benoit, TiMoCN Based Cermets: Part I. Morphology and Phase Composition. *Int. J. Refract. Met. Hard Mater.* **21**, 37–46 (2003)
20. J. Zackrisson, H.O. Andrén, and U. Rolander, Development of Cermet Microstructures during Sintering. *Metall. Mater. Trans. A* **32**, 85–94 (2001)
21. Y. Zheng, W. Xiong, W. Liu, W. Lei, and Q. Yuan, Effect of Nano Addition on the Microstructures and Mechanical Properties of Ti(C, N)-Based Cermets. *Ceram. Int.* **31**, 165–170 (2005)
22. G. Dong, J. Xiong, J. Chen, Z. Guo, W. Wan, C. Yi, and H. Chen, Effect of WC on the Microstructure and Mechanical Properties of Nano Ti(C, N)-Based Cermets. *Int. J. Refract. Met. Hard Mater.* **35**, 159–162 (2012)

23. D. Mari, S. Bolognini, G. Feusier, T. Cutarda, T. Viatteb, and W. Benoita, TiMoCN Based Cermets: Part II. Microstructure and Room Temperature Mechanical Properties. *Int. J. Refract. Met. Hard Mater.* **21**, 47–53 (2003)
24. Z. Gao and S. Kang, A Modeling Investigation for Pseudo-ternary (Ti, Mo, W)(CN) Solid-Solution: Thermodynamic and Elastic Properties. *Comput. Mater. Sci.* **83**, 51–56 (2014)
25. J. Wang, Y. Liu, J. Ye, S. Ma, and J. Pang, The Fabrication of Multi-core structure Cermets Based on (Ti, W, Ta)CN and TiCN Solid-Solution Powders. *Int. J. Refract. Met. Hard Mater.* **64**, 294–300 (2017)
26. H. Kwon, S.A. Jung, C.Y. Suh, K.M. Roh, W. Kim, and J. Kim, Highly Toughened Dense TiC–Ni Composite by In Situ Decomposition of (Ti, Ni)C Solid Solution. *Ceram. Int.* **41**, 4656–4661 (2015)